Chemistry–A European Journal
Research Article
doi.org/10.1002/chem.202202291
Chemistry Europe
European Chemical Societies Publishing
www.chemeurj.org

Photostable NIR-II Pigments from Extended Rylenecarboximides

Ze-Hua Wu,[a, b] Hans Reichert,[c] Helmut Reichelt,[c] Thomas Basché,[b] and Klaus Müllen*[a, b]

Abstract: A series of near-infrared (NIR) organic absorbers, named **FNs** and **FPs**, have been obtained with absorption maxima from 870 nm to 1100 nm and thus falling into the attractive second near-infrared region (NIR-II). The synthesis of their extended aromatic cores utilized an initial arylamination between 4-aminonaphthalene-1,8-dicarboximide (**NMI-NH$_2$**) or 9-aminoperylene-3,4-dicarboximide (**PMI-NH$_2$**) with chloro-substituted 9,10-anthraquinones followed by a novel base-induced cyclodehydrogenation. A NIR-II pigment, compound **FPP**, was obtained through de-alkylation of a soluble precursor. The synthesis of this photostable pigment is high-yielding and avoids column chromatographic purification which is important for many applications.

Introduction

Research into organic near-infrared (NIR) absorbers has attracted attention due to their many optoelectronic[1] and biological applications.[2] Recently, increasing efforts are directed towards the second near-infrared region (NIR-II, 1000–1700 nm) which offers special advantages such as deep penetration depth in photothermal therapy[3] and high signal-to-noise ratio in sensing.[4] Organic NIR absorbers are more favorable than their inorganic counterparts in view of their tunable chemical structures, solution processability and biological compatibility.[5] Nevertheless, the number of organic molecules with NIR-II absorption is still limited.[6–8]

The main bottleneck of organic NIR-II absorbers in applications is the limited photostability during, both, manufacturing and operation.[9] Design strategies towards organic NIR absorbers rest upon extending π-conjugation and enhancing intramolecular charge transfer.[10] The high-lying HOMO energies resulting from the presence of electron donors, however, can cause undesired photooxidation upon irradiation.[11] In some applications, the photostability can be improved by processing techniques. Thus, in photothermal therapy, NIR absorbers are encapsulated into nanoparticles via co-assembly with biocompatible polymers,[12] while in organic photovoltaics (OPVs) an inverted device structure is employed.[13]

Common pigments such as quinophthalone[14] and quinacridone[15] which are completely or nearly insoluble in their matrix systems exhibit light and weather fastness as well as stability against chemical decomposition. These outstanding properties are closely related to the formation of a dense polymer-like molecular packing[16] induced by strong intra- or intermolecular hydrogen bonds and π-π interactions.[17] These give rise to high lattice energies and provide barriers against solvent and oxygen penetration.[18]

Thus, combining NIR-II absorption and pigment stability becomes mandatory, but defines additional requirements in terms of synthesis and purification. Herein, we developed a series of new NIR dyes based on anthraquinone, named as **FNs** and **FPs** (as shown in Figure 1). Their absorption maxima (λ_{max}) cover an attractive wavelength domain from 870 nm to 1100 nm, extending far into the NIR-II. The synthetic protocol

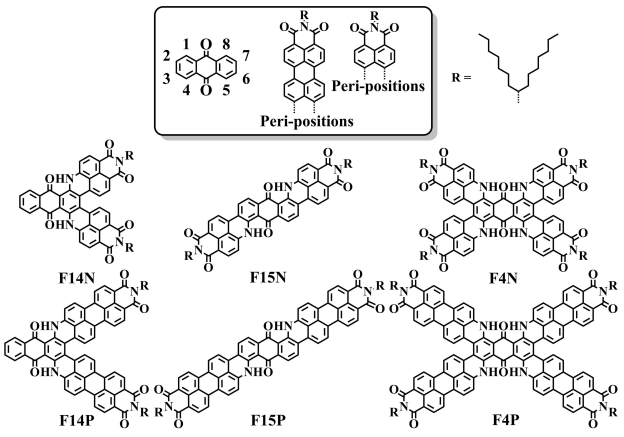

Figure 1. Molecular structures of **FPs** and **FNs** in this work.

[a] *Dr. Z.-H. Wu, Prof. Dr. K. Müllen*
Max Planck Institute for Polymer Research
Ackermannweg 10, 55128 Mainz (Germany)
E-mail: muellen@mpip-mainz.mpg.de
[b] *Dr. Z.-H. Wu, Prof. Dr. T. Basché, Prof. Dr. K. Müllen*
Institute for Physical Chemistry
Johannes Gutenberg University Mainz,
Duesbergweg 10–14, 55128 Mainz (Germany)
[c] *Dr. H. Reichert, Dr. H. Reichelt*
BASF Schweiz AG,
Basel, Rheinfelderstrasse 4133 Schweizerhalle (Switzerland)

Supporting information for this article is available on the WWW under https://doi.org/10.1002/chem.202202291

comprises three steps: i) Connecting naphthalene-1,8-dicarboximide (NMI) and perylene-3,4-dicarboximide (PMI), respectively, to an anthraquinone core through Buchwald–Hartwig C–N coupling; ii) Extending the conjugation by fusing the peri-positions of NMI and PMI with anthraquinone via base-promoted dehydrogenative cyclization; iii) Employing a de-alkylation reaction to transform the **F15P** dye into a pigment. Importantly from an application point of view, the entire synthetic procedure is high-yielding without column chromatographic purification and thus prone of straightforward upscaling.

Results and Discussion

As depicted in Scheme 1, a Buchwald–Hartwig C–N coupling connected 4-aminonaphthalene-1,8-carboximide (**NMI-NH$_2$**) with 1,4-dichloroanthraquinone, 1,5-dichloroanthraquinone and 1,4,5,8-tetrachloroanthraquinone, respectively, to provide the coupling products **14N**, **15N** and **4N**. Due to the electron-withdrawing character of the dicarboximide group,[19] the nucleophilicity of the amino group in **NMI-NH$_2$** is significantly reduced.[20,21] Thus, the commonly used ligands of the metal catalyst such as 2,2′-bis(diphenylphosphino)-1,1′-binaphthalene (BINAP), dicyclohexyl[2′,4′,6′-tris(propan-2-yl)[1,1′-biphenyl]-2-yl]phosphane (Xphos) and tri-*tert*-butylphosphine (*t*-Bu$_3$P) are not applicable when targeting the C–N coupling of the electron deficient aromatic amines. After screening, the coupling reactions of **NMI-NH$_2$** were successfully conducted with 2-(dicyclohexylphosphino)-3,6-dimethoxy-2,4,6′-triisopropyl-1,1′-biphenyl (Brettphos) and its precatalyst.[22] The highly efficient C–N-bond formation allowed one to avoid purification by column chromatography. Remaining **NMI-NH$_2$** reagent could be readily removed through extraction and precipitation in dichloromethane/methanol, furnishing **14N**, **15N** and **4N** in yields of 80%, 85% and 70%, respectively. The next step, a remarkable C–C coupling between the 2,3,6,7-positions of anthraquinone (shown in Scheme 1) and the peri-positions of NMI, can be regarded as a cyclodehydrogenation. Similar processes have been employed in the synthesis of large polycyclic aromatic hydrocarbons and graphene nanoribbons.[23,24] The oxidants used for such fusions of electron-rich oligo- and polyphenylene precursors are inapplicable for the present molecules.[25] Herein, we utilized a base-induced anionic cyclization reaction[26,27] as a complement to the ring fusions performed under acidic and/or oxidizing conditions. The base causes deprotonation and promotes the nucleophilic attack of carbanion intermediates on the adjacent aromatic units followed by oxidation upon exposure to oxygen in the workup. Using potassium carbonate as base, the fused products, **F14N**, **F15N** and **F4N** were obtained in yields of 60%, 65% and 60%, respectively. Here again, the workup circumvents column chromatography as the base and hydrolysis byproducts can be removed by filtration, washing and precipitation in dichloromethane/methanol.

As described in Scheme 2, the analogous protocol for the C–N coupling of 9-aminoperylene-3,4-carboximide (**PMI-NH$_2$**) with 1,4-, 1,5- and 1,4,5,8-chloro substituted anthraquinones afforded **14P**, **15P** and **4P**, respectively, in yields of 80%, 70% and 60%. In these cases, ring fusion was achieved by base-promoted dehydrogenative cyclization with 1,5-diazabicyclo(4.3.0)non-5-ene (DBN) and potassium *tert*-butoxide (*t*BuONa) furnishing the fused products, **F14P**, **F15P**, and **F4P** in yields of 70%, 70%, and 60%, respectively.

The final products **FNs** and **FPs** as well as their precursors can be dissolved in common solvents such as dichloromethane and tetrahydrofuran to give concentrations above 2 mg/mL. Their molecular structures were fully characterized by nuclear magnetic resonance (NMR) spectroscopy, high-resolution matrix-assisted laser desorption/ionization time-of-flight mass spectrometry (HR MALDI-TOF MS), combustion analysis and Fourier transform infrared spectroscopy (FTIR) spectroscopy. In

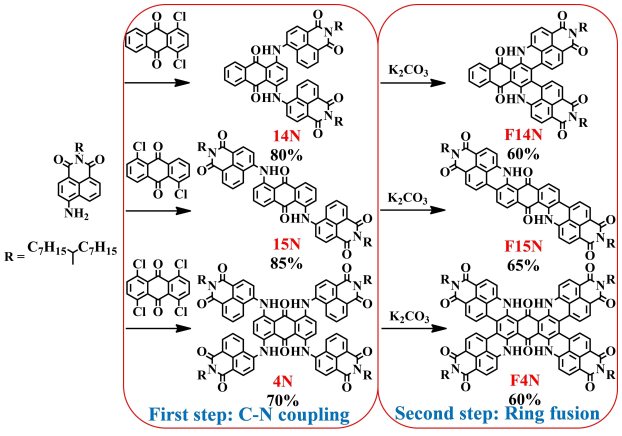

Scheme 1. Synthetic route for **FNs**. Reagents and conditions of C–N coupling: Brettphos, Brettphos Pd G1, Cs_2CO_3, toluene, 110 °C, 12 h, 80% for **14N**, 85% for **15N**, 70% for **4N**. Reagents and conditions of dehydrogenative cyclization reaction: K_2CO_3, ethanolamine, 130 °C, 24 h, 60% for **F14N**, 65% for **F15N**, 60% for **F4N**.

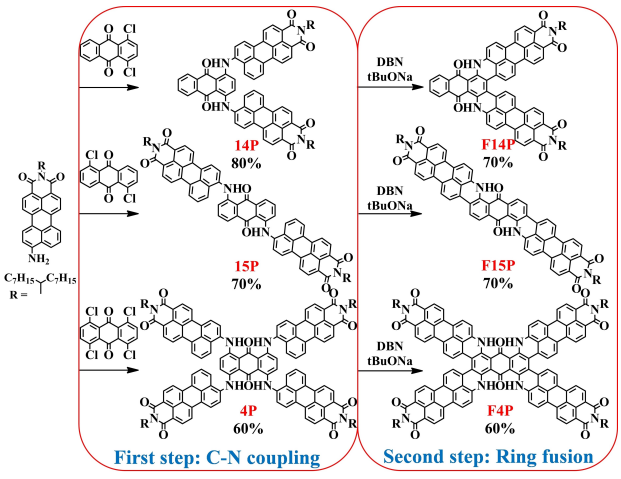

Scheme 2. Synthetic route for **FPs**. Reagents and conditions of C–N coupling: Brettphos, Brettphos Pd G1, Cs_2CO_3, toluene, 110 °C, 12 h, 80% for compound **14P**, 70% for **15P**, 60% for **4P**. Reagents and conditions of dehydrogenative cyclization reaction: DBN, *t*BuONa, Diglyme, 130 °C, 24 h, 70% for **F14P** and **F15P**, 60% for **F4P**.

order to suppress the - still existing - strong aggregation due to π-π interaction of these conjugated compounds, ^{1}H NMR spectra have to be recorded at elevated temperature (130 °C) in *o*-dichlorobenzene-d_4 or 1,1,2,2-tetrachlorethane-d_2 with concentrations less than 2 mg/mL. MALDI-TOF MS analysis firmly proved the removal of 4 protons in **F14N**, **F14P**, **F15N** and **F15P** as well as 8 protons in **F4N** and **F4P** upon multiple C–C bond formation and corroborated the complete dehydrogenation. The observed isotopic distribution patterns are fully consistent with the simulated mass spectra.

The optical properties of **FNs** and **FPs** were studied by UV-vis-NIR absorption spectrometry in tetrahydrofuran (THF). As shown in Figure 2, the absorption maxima (λ_{max}) of **F14N**, **F15N**, **F4N**, **F14P**, **F15P** and **F4P** are located at 872, 720, 1286, 1028, 900 and 1023 nm, respectively, which can be assigned to the HOMO→LUMO electronic transition based on time-dependent density functional theory (TD-DFT) calculations (Table S2). In comparison with the λ_{max} of their corresponding precursors in the range of 521 to 729 nm (Figure S1), prominent bathochromic shifts by more than 200 nm are demonstrated, reflecting the extremely useful cyclodehydrogenation.[28] As displayed in Figure S3, **F4N** exhibits the largest solvatochromism. Its λ_{max} at 1286 nm in THF is red-shifted to 1310 nm in toluene with concomitant increase of absorbance. The solvent-dependent absorption indicates the n-π* electron transition characteristics[29] of λ_{max}, as originating from the electrostatic interactions[30] between solvents and nitrogen lone pair electrons[30] on the 1,4,5,8-positions of anthraquinone.

The electrochemical properties of the title compounds were estimated by cyclic voltammetry (CV) in THF. The HOMO and LUMO energy levels (E_{HOMO} and E_{LUMO}) were calculated from the oxidation and reduction onsets which were calibrated using ferrocene/ferrocene$^+$ (Fc^+/Fc) as standard. As summarized in Table S1, **FNs** and **FPs** exhibit low-lying E_{LUMO} in the range of −3.65 to −4.18 eV as well as energy gaps (E_{gap}) in the range of 1.43 to 0.83 eV. These values indicate a potential as narrow-gap acceptors in organic photovoltaics to extend the absorption spectral range into the NIR region and reduce energy loss during charge generation.[32]

The important photostability of the chromophores was tested by monitoring the diffuse reflectance spectrum of thoroughly ground solid powders upon irradiation with sunlight under ambient atmosphere for 14 days. The light fastness of all soluble NIR-II dyes was screened in order to select the most promising candidate for subsequent pigment formation. As illustrated in Figure S7, **F15P** demonstrates the highest photostability by displaying a 15% decrease of reflectance at λ_{max} after 1 day of irradiation without any further changes upon further irradiation. The initial decay can be attributed to the photodissociation of small-sized amorphous particles while, the remaining particles demonstrate good light fastness due to dense molecular packing.[33]

Thus, **F15P** was used for pigment formation by de-alkylation. Herein, 4-*tert*-butyl-α-methylbenzylamine was employed as side group at the imide of PMI which could be readily removed by treatment with boronic tribromide (BBr_3) at 0 °C in nearly quantitative yield. As depicted in Figure 3a, the latent pigment (compound **1**) was obtained in 60% yield following the same synthetic protocol as for **F15P**. Subsequent de-alkylation with BBr_3 afforded the pigment, that is compound **FPP**, in 80% yield. The molecular structure was characterized by MALDI-TOF MS, combustion analysis and FTIR spectroscopy. As becoming obvious from the high-resolution mass spectrum of **FPP** (Figure 3b), the intense signal at 872.1736 is in good agreement with corresponding calculated molecular mass of 872.1696, and the observed isotopic distribution patterns are fully consistent with the calculated spectrum. The FTIR spectrum of pigment **FPP** (Figure 3c) displays two peaks of N–H

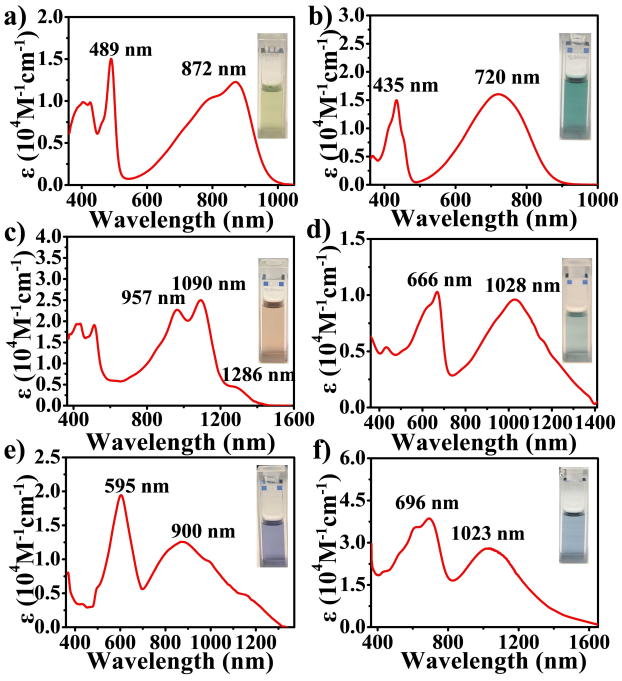

Figure 2. UV-vis-NIR absorption spectra of a) **F14N**, b) **F15N**, c) **F4N**, d) **F14P**, e) **F15P** and f) **F4P**. The photographs of solutions (1×10^{-4} M in tetrahydrofuran) are inserted in corresponding absorption spectra.

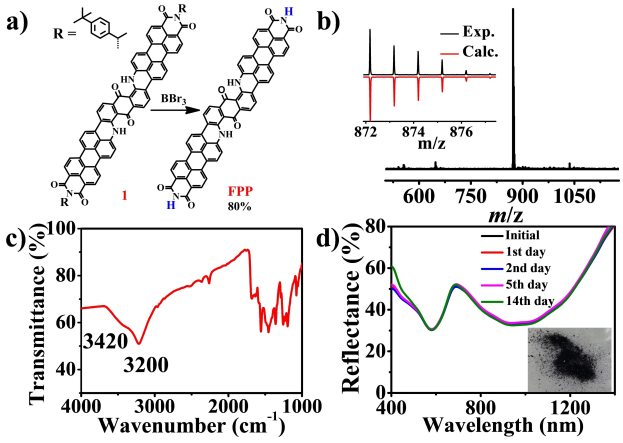

Figure 3. a) De-alkylation reaction from latent pigment **1** to **FPP**. Reagents and condition: BBr_3, dichloromethane, 0 °C, 12 h. b) MALDI-TOF MS of **FPP**. Inset: experimental and theoretical isotopic distribution patterns. c) FTIR spectrum of **FPP**. d) Diffuse reflectance spectrum of **FPP** upon irradiation with sunlight for 14 days under ambient atmosphere. Inset: the photograph of solid powder.

stretching vibrations at 3200 and 3420 cm^{-1}. The former (broader) band suggests intermolecular hydrogen bonding at the carboximide functions.[34] This is supported by a comparison with the latent pigment **1** (Figure S6) which only exhibits the N–H vibration band at 3420 cm^{-1} of the amino group on the anthraquinone.[35] The resulting close packing in **FPP** was confirmed by its diffuse reflectance spectrum in the solid state which exhibits a red-shifted λ_{max} at 930 nm (Figure 3d). After irradiation with sunlight under ambient atmosphere for 14 days, no attenuation of reflectance in the NIR-II region was observed, revealing the excellent light fastness of **FPP**. Under the same test condition, the commercially available NIR dye, indocyanine green exhibited 8–16% attenuation of reflectance at λ_{max} per day (Figure S7) which indicates the superior photostability of **FPP**.

Conclusion

We have demonstrated an efficient strategy towards a series of new NIR dyes based on anthraquinone with absorption peaks ranging from 870 nm to 1100 nm. A **FPP** pigment with NIR-II absorption was developed through a de-alkylation reaction. The resulting intermolecular N–H···O=C hydrogen bond leads to dense packing and brings about excellent light fastness. This pigment holds great potential not only as colorant, but also in high-end applications with critical photostability requirements such as security printing, heat shielding and laser welding. The entire synthetic procedure is efficient without column chromatographic purification and thus prone of large-scale production. The reaction conditions of C–N coupling and cyclodehydrogenation in this work will be applicable to other electron-deficient structures such as 1,4-naphthoquinone and 6,13-pentacenequinone. Further studies on even more extended rylene homologues are ongoing in our group.

Acknowledgements

KM gratefully acknowledges support of this work by the Gutenberg Research College of the Johannes Gutenberg University, Mainz, and by the Max Planck Society through an Emeritus Group. Open Access funding enabled and organized by Projekt DEAL.

Conflict of Interest

The authors declare no conflict of interest.

Data Availability Statement

The data that support the findings of this study are available from the corresponding author upon reasonable request.

Keywords: cyclodehydrogenation · photostability · pigment · rylenecarboximide · second near-infrared

[1] R. Muñoz-Mármol, F. Gordillo, V. Bonal, J. M. Villalvilla, P. G. Boj, J. A. Quintana, A. M. Ross, G. M. Paternò, F. Scotognella, G. Lanzani, A. Derradji, J. C. Sancho-García, Y. Gu, J. Wu, J. Casado, M. A. Díaz-García, *Adv. Funct. Mater.* **2021**, *31*, 2105073.
[2] C. Liu, S. Zhang, J. Li, J. Wei, K. Müllen, M. Yin, *Angew. Chem. Int. Ed.* **2019**, *58*, 1638–1642; *Angew. Chem.* **2019**, *131*, 1652–1656.
[3] J. Mu, M. Xiao, Y. Shi, X. Geng, H. Li, Y. Yin, X. Chen, *Angew. Chem.* **2022**, *134*, e202114722.
[4] S. Park, K. Fukuda, M. Wang, C. Lee, T. Yokota, H. Jin, H. Jinno, H. Kimura, P. Zalar, N. Matsuhisa, S. Umezu, G. C. Bazan, T. Someya, *Adv. Mater.* **2018**, *30*, 1802359.
[5] B. Xie, Z. Chen, L. Ying, F. Huang, Y. Cao, *InfoMat.* **2020**, *2*, 57–91.
[6] W. Shao, Q. Wei, S. Wang, F. Li, J. Wu, J. Ren, F. Cao, H. Liao, J. Gao, M. Zhou, D. Ling, *Mater. Horiz.* **2020**, *7*, 1379–1386.
[7] S. Li, Q. Deng, Y. Zhang, X. Li, G. Wen, X. Cui, Y. Wan, Y. Huang, J. Chen, Z. Liu, L. Wang, C.-S. Lee, *Adv. Mater.* **2020**, *32*, 2001146.
[8] B. Pigulski, K. Shoyama, F. Würthner, *Angew. Chem. Int. Ed.* **2020**, *59*, 15908–15912; *Angew. Chem.* **2020**, *132*, 16042–16046.
[9] Y. Liu, Y. Li, S. Koo, Y. Sun, Y. Liu, X. Liu, Y. Pan, Z. Zhang, M. Du, S. Lu, X. Qiao, J. Gao, X. Wang, Z. Deng, X. Meng, Y. Xiao, J. S. Kim, X. Hong, *Chem. Rev.* **2021**, *122*, 209–268.
[10] B. Xie, Z. Chen, L. Ying, F. Huang, Y. Cao, *InfoMat.* **2020**, *2*, 57–91.
[11] T. Furuyama, Y. Miyaji, K. Maeda, H. Maeda, M. Segi, *Chem. Eur. J.* **2019**, *25*, 1678–1682.
[12] H. Xiang, L. Zhao, L. Yu, H. Chen, C. Wei, Y. Chen, Y. Zhao, *Nat. Commun.* **2021**, *12*, 218.
[13] R. Munir, E. Cieplechowicz, R. M. Lamarche, R. Chernikov, S. Trudel, G. C. Welch, *Adv. Mater. Interfaces* **2022**, *9*, 2101918.
[14] V. Radtke in *High performance pigments,Vol. 19* (Eds.: E. Faulkner, RJ. Schwartz), Wiley-VCH, Weinheim, **2009**, pp. 331–340.
[15] Q. He, M. Worku, H. Liu, E. Lochner, A. J. Robb, S. Lteif, J. S. R. Vellore Winfred, K. Hanson, J. B. Schlenoff, B. J. Kim, B. Ma, *Angew. Chem. Int. Ed.* **2021**, *60*, 2485–2492; *Angew. Chem.* **2021**, *133*, 2515–2522.
[16] E. D. Głowacki, H. Coskun, M. A. Blood-Forsythe, U. Monkowius, L. Leonat, M. Grzybowski, D. Gryko, M. S. White, A. Aspuru-Guzik, N. S. Sariciftci, *Org. Electron.* **2014**, *15*, 3521–3528.
[17] Z. Hao, A. Iqbal, *Chem. Soc. Rev.* **1997**, *26*, 203–213.
[18] J. Mizuguchi, *J. Phys. Chem. A* **2000**, *104*, 1817–1821.
[19] L. Chen, C. Li, K. Müllen, *J. Mater. Chem. C* **2014**, *2*, 1938–1956.
[20] B. P. Fors, D. A. Watson, M. R. Biscoe, S. L. Buchwald, *J. Am. Chem. Soc.* **2008**, *130*, 13552–13554.
[21] A. Collado, D. J. Nelson, S. P. Nolan, *Chem. Rev.* **2021**, *121*, 8559–8612.
[22] D. S. Surry, S. L. Buchwald, *Chem. Sci.* **2011**, *2*, 27–50.
[23] Q. Chen, L. Brambilla, L. Daukiya, K. S. Mali, *Angew. Chem. Int. Ed.* **2018**, *57*, 11233–11237; *Angew. Chem.* **2018**, *130*, 11403–11407.
[24] M. Grzybowski, B. Sadowski, H. Butenschön, D. T. Gryko, *Angew. Chem. Int. Ed.* **2020**, *59*, 2998–3027; *Angew. Chem.* **2020**, *132*, 3020–3050.
[25] L. Chen, C. Li, K. Müllen, *J. Mater. Chem. C* **2014**, *2*, 1938–1956.
[26] T. Sakamoto, C. Pac, *J. Org. Chem.* **2001**, *66*, 94–98.
[27] M. Rickhaus, A. P. Belanger, H. A. Wegner, Scott, L. T. Scott, *J. Org. Chem.* **2010**, *75*, 7358–7364.
[28] C. Kang, K. Jung, S. Ahn, T.-L. Choi, *J. Am. Chem. Soc.* **2020**, *142*, 17140–17146.
[29] F. Meierhofer, F. Dissinger, F. Weigert, J. Jungclaus, K. Müller-Caspary, S. R. Waldvogel, U. Resch-Genger, T. Voss, *J. Phys. Chem. C* **2020**, *124*, 8894–8904.
[30] T. Haldar, S. Bagchi, *J. Phys. Chem. Lett.* **2016**, *7*, 2270–2275.
[31] J. Zhao, X. Zhang, R. Zhu, T. Su, D. L. Phillips, *J. Phys. Chem. B* **2019**, *123*, 3156–3162.
[32] N. Liang, D. Meng, Z. Wang, *Acc. Chem. Res.* **2021**, *54*, 961–975.
[33] A. Nowak-Król, K. Shoyama, M. Stolte, F. Würthner, *Chem. Commun.* **2018**, *54*, 13763–13772.
[34] S. Herbst, B. Soberats, P. Leowanawat, M. Lehmann, F. Würthner, *Angew. Chem. Int. Ed.* **2017**, *56*, 2162–2165.
[35] R. Xue, Y.-P. Zheng, L. Zhang, D.-Y. Xu, D.-Q. Qian, Y.-S. Liu, H.-H. Rao, S.-L. Huang, G.-Y. Yang, *New J. Chem.* **2021**, *45*, 19125–19131.

Manuscript received: July 21, 2022
Accepted manuscript online: July 25, 2022
Version of record online: August 29, 2022